

# Low temperature saturation of phase coherence length in topological insulators

Saurav Islam<sup>1</sup>, Semonti Bhattacharyya<sup>1,2</sup>, Hariharan Nhalil<sup>1</sup>, Mitali Banerjee<sup>1,3</sup>, Anthony Richardella<sup>4</sup>, Abhinav Kandala<sup>4,5</sup>, Diptiman Sen<sup>6</sup>, Nitin Samarth<sup>4</sup>, Suja Elizabeth<sup>1</sup>, Arindam Ghosh<sup>1,7</sup>

<sup>1</sup>*Department of Physics, Indian Institute of Science, Bangalore: 560012.*

<sup>2</sup>*School of Physics and Astronomy, Monash University, VIC 3800, Australia.*

<sup>3</sup>*Department of Physics, Columbia University, New York, NY 10027, USA.*

<sup>4</sup>*Department of Physics, The Pennsylvania State University, University Park, Pennsylvania 16802 – 6300, USA.*

<sup>5</sup>*IBM T.J. Watson Research Center, Yorktown Heights, New York 10598, USA.*

<sup>6</sup>*Center for High Energy Physics, Indian Institute of Science, Bangalore: 560012. and*

<sup>7</sup>*Center for Nanoscience and Engineering, Indian Institute of Science, Bangalore: 560012.\**

Implementing topological insulators as elementary units in quantum technologies requires a comprehensive understanding of the dephasing mechanisms governing the surface carriers in these materials, which impose a practical limit to the applicability of these materials in such technologies requiring phase coherent transport. To investigate this, we have performed magneto-resistance (MR) and conductance fluctuations (CF) measurements in both exfoliated and molecular beam epitaxy grown samples. The phase breaking length ( $l_\phi$ ) obtained from MR shows a saturation below sample dependent characteristic temperatures, consistent with that obtained from CF measurements. We have systematically eliminated several factors that may lead to such behavior of  $l_\phi$  in the context of TIs, such as finite size effect, thermalization, spin-orbit coupling length, spin-flip scattering, and surface-bulk coupling. Our work indicates the need to identify an alternative source of dephasing that dominates at low  $T$  in topological insulators, causing saturation in the phase breaking length and time.

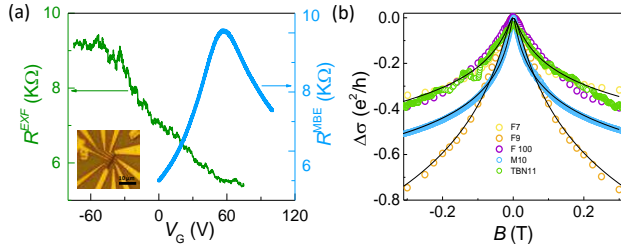


Figure 1. **Quantum transport in topological insulator FETs.** (a) Typical  $R - V_G$  for exfoliated TI ( $R^{EXF}$ ) TBN11 and epitaxially grown TI ( $R^{MBE}$ ) M10 at 20mK. Inset: optical micrograph of a typical exfoliated TI FET (b) Weak-anti-localisation behavior observed in different samples at  $T = 300$  mK. The solid black lines are fits to the data using Eq. 1.

Topological insulators (TIs) [1–4] are a new class of materials characterized by the presence of gapless and linearly dispersing metallic surface states present in the bulk band gap due to non-trivial topology of the bulk band structure. The surface carriers are prohibited from back-scattering against non-magnetic impurities and exhibit a plethora of fundamentally important effects such as spin-momentum locking, hosting Majorana fermions in the presence of a superconductor, topological magnetoelectric effect, and quantum anomalous Hall effect [1, 5]. The topological protection of these surface states makes these materials a strong contender for the building blocks of qubits, which require long phase coherence length ( $l_\phi$ )

for error tolerant quantum computation. Hence, it is critical to understand the mechanisms responsible for dephasing or decoherence, which is equivalent to loss of information, in the surface states of TIs. The most common dephasing mechanism in TIs at low temperature ( $T$ ) has been known to be electron-electron interaction [6–10], and the coupling of the surface states to localized charged puddles in the bulk [11]. Li et al. have demonstrated that electron-phonon interaction is also required to explain the dependence of  $l_\phi$  on  $T$  [12]. Although theoretically, all these mechanisms lead to a diverging  $l_\phi$  with decreasing  $T$  [6, 7, 13, 14], experimentally, the increase of  $l_\phi$  with reducing  $T$  is often followed by its saturation for  $T \leq 2 - 5$  K [11, 12, 15, 16]. The saturation of  $l_\phi$  at a finite value instead of its divergence for  $T \rightarrow 0$  K, which is predicted for electron-electron or electron-phonon interactions, has been a matter of active discourse [14, 17–28].

In this report, we have inspected the factors that can lead to the saturation of  $l_\phi$  in TIs by measuring both gate-voltage ( $V_G$ ) and time ( $t$ )-dependent conductance fluctuations and magneto-resistance (MR) [27, 29–36]. Conductance fluctuations result from the quantum interference of different electron trajectories, manifested as sample specific, aperiodic fluctuations in the conductance due to varying disorder configuration, Fermi energy, and magnetic field; such fluctuations have been used as a tool to probe the presence of time-reversal symmetry (TRS) breaking disorders, since the saturation of  $l_\phi$  at low  $T$  is often attributed to spin-flip scattering processes. The magnitude of the conductance fluctuations  $\langle \delta G^2 \rangle$ , however, shows a factor of two reduction upon application of a perpendicular magnetic field ( $B_\perp$ ), implying that TRS is intrinsically preserved in these systems. Addi-

\* isaurav@iisc.ac.in; SI and SB contributed equally

Table I. **Details of measured devices:** The thickness, substrate, composition, saturation value of temperature ( $T^{sat}$ ), and saturation value of phase breaking length ( $l_\phi^{sat}$ ) for various devices that been investigated is provided in the table.

Sample	Thickness	Substrate	Composition	$T^{sat}$	$l_\phi^{sat}$
F7	7	SiO <sub>2</sub> /Si++	Bi <sub>1.6</sub> Sb <sub>0.4</sub> Te <sub>2</sub> Se	~ 2 K	200 nm
F100	100	SiO <sub>2</sub> /Si++	Bi <sub>1.6</sub> Sb <sub>0.4</sub> Te <sub>2</sub> Se	~ 2 K	150 nm
F9	9	SiO <sub>2</sub> /Si++	Bi <sub>1.6</sub> Sb <sub>0.4</sub> Te <sub>2</sub> Se	~ 2 K	NA
TBN11	11	Boron nitride	Bi <sub>1.6</sub> Sb <sub>0.4</sub> Te <sub>2</sub> Se	~ 2 K	190 nm
M10	10	STO	(Bi,Sb) <sub>2</sub> Te <sub>3</sub>	~ 300 mK	2000 nm

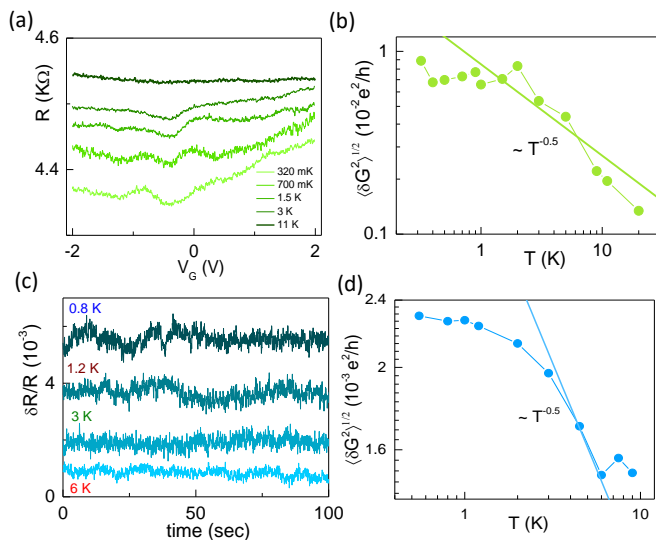


Figure 2. **Conductance fluctuations measurements.** (a)  $R$  vs  $V_G$  for different  $T$  for device F100 in a 4 V window, used to extract  $\langle \delta G^2 \rangle$ . (b)  $\langle \delta G^2 \rangle^{1/2}$  as a function of  $T$  which shows a saturation below  $T < 2$  K for the device F100. Above 2 K,  $\langle \delta G^2 \rangle^{1/2} \propto 1/T^{0.5}$ . (c) Normalized resistance fluctuations in the time domain for different  $T$  used for calculation of P.S.D (d) Noise magnitude as a function of  $T$  also showing a saturation below  $T < 2$  K. Above 2 K,  $\langle \delta G^2 \rangle^{1/2} \propto 1/T^{0.5}$ .

tionally, at different gate voltages,  $\langle \delta G^2 \rangle$  displays a saturation for  $T < 2$  K, even in the presence of a large  $B_\perp$  which suppresses spin-spin scattering; this implies that neither magnetic impurities nor the coupling of the surface and the bulk impurity states is responsible for the saturation. Our experiment suggests an unconventional mechanism that saturates  $l_\phi$  in TIs, possibly arising from unscreened Coulomb fluctuations from the charged disorders present in the bulk [11].

The field effect devices investigated in this paper were fabricated from both exfoliated and molecular beam epitaxy (MBE) grown TIs. To fabricate the former, the TI Bi<sub>1.6</sub>Sb<sub>0.4</sub>Te<sub>2</sub>Se (BSTS) (purity of the starting elements Bi, Te, Sb, Se  $\geq 4$ N) was exfoliated from a single crystal onto a SiO<sub>2</sub>/Si++ substrate with the 285 nm thick SiO<sub>2</sub> acting as the back gate dielectric inside a glove box [37]. This was followed by standard electron-beam lithography and sputtering of 100 nm Au to form

the source-drain contacts (inset of Fig. 1(a)). The details of the devices measured are provided in Table. I. In sample TBN11, the TI flake was transferred onto an atomically flat boron nitride (BN) substrate to reduce the effect of charged traps and dangling bonds of SiO<sub>2</sub> on the electrical transport [38], followed by lithography and metallization. The quarternary alloy BSTS offers a reduced bulk number density due to compensation doping, resulting in a higher percentage of surface transport [37]. The exfoliated samples were covered with PMMA (poly(methylmethacrylate)) during the entire measurement cycle to prevent oxidation and subsequent degradation of the surface quality. The large area (0.5 mm  $\times$  1 mm) sample (M10) was fabricated from thin (thickness,  $d = 10$  nm) (Bi,Sb)<sub>2</sub>Te<sub>3</sub> (BST) (purity of starting elements was 5N for Bi, 5N for Sb and 6N for Te,) grown by molecular beam epitaxy (MBE) on (111) SrTiO<sub>3</sub> (STO) substrate and mechanically etched into a Hall bars with a metallic coating of Indium at the back, that was used as a back gate electrode [39, 40]. Resistivity measurements were performed in a low-frequency four-probe AC configuration in a pumped He-3 system (base  $T = 320$  mK) and in a dilution refrigerator (base  $T = 20$  mK).

Preliminary electrical transport characteristics in the exfoliated device TBN11 (at  $T = 20$  mK) and the MBE-grown device (at 20 mK) are shown in Fig. 1(a). The  $R$ - $V_G$  data indicates that at  $V_G = 0$  V, TBN11 is intrinsically electron doped and M10 is intrinsically hole doped. Whereas M10 shows a clear graphene like ambipolar transport with a Dirac point at 60 V, which could be achieved due to the high dielectric constant of the STO at low  $T$  ( $\epsilon_r \sim 44000$  at 5 K) [40], TBN11 shows a clear signature of an electron-hole puddle regime at  $V_G = -60$  V. The estimated value of intrinsic number density at  $V_G = 0$  V are  $-2.9 \times 10^{13} \text{ m}^{-2}$  and  $9 \times 10^{13} \text{ m}^{-2}$  respectively. The quantitative difference of the  $V_G$ -dependent characteristics here indicates dominance of different types of disorder species in the samples, owing to different processes of synthesis, fabrication, and composition. The n-doping in BSTS mostly comes due to Se vacancies, the most likely probable cause of p-doping in the epitaxially grown samples is the presence of anti-site defects.

Fig. 1(b) shows weak anti-localization (WAL) for different samples, which is characterized by a cusp in the quantum correction to conductivity  $\Delta\sigma$  at  $B = 0$  T, and is a result of  $\pi$  Berry phase in topological insula-

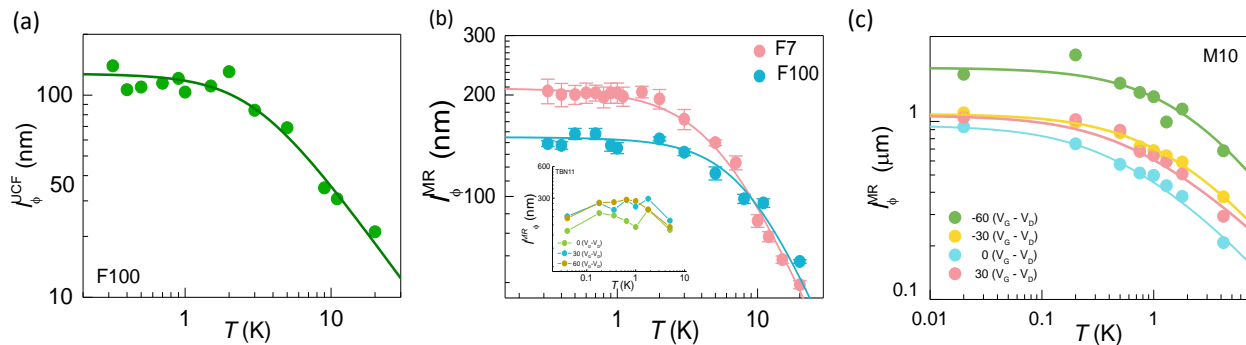


Figure 3. **Saturation of phase breaking length** ( $l_\phi$ ). (a)  $l_\phi$  vs  $T$  extracted from  $T$ -dependence of  $\langle\delta G^2\rangle$  using Eq. 2 for device F100. The solid line is fit according to Eq. 4. (b)  $l_\phi$  vs  $T$  extracted from  $T$ -dependence of WAL data using Eq. 1 for exfoliated samples F7 and F100 which shows a saturation below  $T < 3$  K. The solid lines are fits to Eq. 1. Inset shows  $l_\phi$  vs  $T$  extracted from  $T$ -dependence of WAL data for sample TBN11, which also shows a saturation. (c)  $l_\phi$  vs  $T$  for different  $V_G$  extracted from  $T$ -dependence of WAL data using Eq. 1 for epitaxially grown TI M10 which shows a saturation below  $T < 300$  mK. The solid lines are fits to Eq. 3.

tors. The magneto-conductance data can be fitted with the Hikami-Larkin-Nagaoka (HLN) expression for diffusive metals with high spin-orbit coupling ( $\tau_\phi \gg \tau_{so}, \tau_e$ ) [29, 41]:

$$\Delta\sigma = -\alpha \frac{e^2}{\pi h} \left[ \psi \left( \frac{1}{2} + \frac{B_\phi}{B} \right) - \ln \left( \frac{B_\phi}{B} \right) \right] \quad (1)$$

where  $\tau_\phi$ ,  $\tau_{so}$ ,  $\tau_e$  are the phase coherence or dephasing time, spin-orbit scattering time and elastic scattering time respectively,  $\psi$  is the digamma function and  $B_\phi$  is the phase breaking field. Here  $\alpha$  and  $B_\phi$  are fitting parameters. The phase coherence length  $l_\phi^{MR}$  can be extracted using  $l_\phi^{MR} = \sqrt{\hbar/4eB_\phi}$  and the value of  $\alpha$  gives an estimate of the number of independent conducting channels in the sample (See supplementary information).

The magnitude of gate voltage dependent conductance fluctuations  $\langle\delta G^2\rangle$ , has been evaluated by using a method similar to Ref. [16, 35, 42] by varying the chemical potential with the back gate voltage in steps of 5 mV over a small window of 4 V.  $\langle\delta R^2\rangle$  is extracted from  $R - V_G$  by fitting the data with a smooth polynomial curve.  $\langle\delta G^2\rangle$  is then obtained using the relation:  $\langle\delta G^2\rangle = \langle\delta R^2\rangle/\langle R\rangle^4$  ( $\langle\delta R^2\rangle$  is extracted from the variance of the residual). As shown in Fig. 2(a) for a typical 4 V window, the fluctuations are aperiodic yet reproducible but weaken with increasing  $T$ . The  $T$ -dependence of the standard deviation  $\langle\delta G^2\rangle^{\frac{1}{2}}$ , at  $V_G = 0$  V (center of the corresponding window) for F100 in Fig. 2(b) shows two distinctly different regions. Above  $T > 2$  K,  $\langle\delta G^2\rangle^{\frac{1}{2}} \propto T^{-0.5}$ , which is expected from the  $T$ -dependence of  $l_\phi \propto T^{-0.5}$  and the number of active scatterers ( $n_s \propto T$ ) [16].  $\langle\delta G^2\rangle^{\frac{1}{2}}$ , however, saturates for  $T < 2$  K.

Conductance fluctuations due to changes in the disorder configuration were detected by measuring the normalized noise magnitude, defined as  $\frac{\langle\delta G^2\rangle}{\langle G^2\rangle} = \frac{[S_V df]}{V^2}$

where  $S_V/V^2$  is the normalized power spectral density (P.S.D.) of the time-dependent signal, in an AC-four probe Wheatstone bridge technique ([32, 43]). The normalized time-dependent fluctuations in resistance,  $(\delta R/R)$  for various temperatures ( $0.3 \text{ K} \leq T \leq 6 \text{ K}$ ) is shown in Fig. 2(c).  $\langle\delta G^2\rangle^{\frac{1}{2}}$  extracted from the P.S.D. of time-dependent conductance fluctuations is plotted as a function of  $T$  in Fig. 2(d) and is found to show a saturation below  $T = 2$  K, which is consistent with the behavior of  $\langle\delta G^2\rangle^{\frac{1}{2}}$  obtained from the  $V_G$ -dependence. The order of magnitude difference is caused due to integration of the signal over a finite frequency window as well as the sensitivity of resistance changes to individual defect movements [36, 44, 45].

The phase breaking length,  $l_\phi$  extracted from  $\langle\delta G^2\rangle^{\frac{1}{2}}$ - $T$  data (Fig. 2(a)) using the expression [46, 47]

$$\langle\delta G^2\rangle \simeq \left(\frac{3}{\pi}\right) \left(\frac{e^2}{h}\right)^2 \left(\frac{l_\phi}{L}\right)^2 \quad (2)$$

is shown in Fig. 3a. Since  $\langle\delta G^2\rangle \propto l_\phi^2$ , any saturation obtained from time or gate voltage-dependence should also be reflected in the saturation of  $l_\phi$ , obtained directly from MR measurements. The values of  $l_\phi$  extracted from MR data similar to Fig. 1(b), as a function of  $T$  for the exfoliated samples F100 and F7 is shown in Fig. 3(b). We find that  $l_\phi$  obtained from two different methods,  $l_\phi^{MR}$  and  $l_\phi^{UCF}$  (extracted from Eq. 1 and Eq. 2 respectively) show similar trends with  $T$ , first increasing with decreasing  $T$ , followed by a saturation below  $T \sim 2$  K, thus discarding the possibility of the saturation to be an artifact. The discrepancies in the values of  $l_\phi^{MR}$  and  $l_\phi^{UCF}$  are within uncertainties of the prefactor of Eq. 2 [46–48]. The higher value of  $l_\phi$  for F7 compared to F100 can be due to enhanced dephasing due to trapping-detrapping processes in the bulk, since the thickness of F100 is much larger than that of F7.

For a quantitative understanding,  $l_\phi$ - $T$  data (Fig. 3 (a-b)) has been fitted with the expression commonly used to fit the  $l_\phi$ - $T$  data in 2D diffusive systems [12, 14].

$$l_\phi = \frac{1}{(A_0 + A_1 T + A_2 T^2)^{0.5}} \quad (3)$$

Here,  $l_\phi \propto T^{-0.5}$ , and  $l_\phi \propto T^{-1}$  are the respective contributions from electron-electron (e-e) and electron-phonon (e-ph) scattering.  $A_1$ ,  $A_2$  are fitting parameters and  $A_0 = \frac{1}{l_{\phi 0}^2}$ , the saturation value of  $l_\phi$ . In 2D systems, although e-e interactions are the dominant source of dephasing at low  $T$  and have been adequate to describe dephasing in graphene [14, 49, 50], and in some reports of TI [13, 51], e-ph interaction cannot be neglected for TI because of the vicinity of the bulk to the surface states [11, 12]. However, instead of saturation, these two mechanisms lead to a diverging  $l_\phi$  at low  $T$ . The saturation of  $l_\phi$  has also been obtained in device TBN11, where the TI has been transferred onto a boron nitride substrate (Fig. 3b). The atomically flat boron nitride (thickness  $d = 14$  nm) prevents trapping-detrapping that is commonly observed between the channel and the SiO<sub>2</sub> substrate, thus reducing any dephasing due to electromagnetic fluctuations induced by potential traps present in SiO<sub>2</sub>.

The saturation of  $l_\phi$  is often attributed to (a) finite size effects, where  $l_\phi$  becomes comparable to  $L$ , the length of the sample, (b) saturation of electron temperature due to heating from external sources [14], (c) spin-orbit scattering length becoming comparable to the phase breaking length [17], and (d) magnetic impurities or local magnetic moment [22, 24, 25]. We have systematically explored the possibility of saturation arising from any of the above reasons. To probe the effect of finite size, we have performed MR measurements on M10 with a channel length of 1 mm which is three orders of magnitude more than the saturated value of  $l_\phi$ . The  $l_\phi$  extracted from magneto-conductance data using Eq. 1 also shows a similar saturation for  $T < 300$  mK for all  $V_G$ 's. The saturation obtained in the large area sample, indicates that finite-size effects at low  $T$  is not the cause of the observed behavior of  $l_\phi$ . Another important factor for the saturation is thermalization, where the electron  $T_e$  can be much higher than the lattice temperature  $T_L$ . For extracting  $T_e$  accurately in our He-3 system, we have measured and analyzed the  $T$  dependence of Shubnikov-de Haas oscillations using GaAs/Al<sub>0.33</sub>Ga<sub>0.66</sub>As hetero-structure to ensure that down to  $T = 0.3$  K,  $T_e$  matches  $T_L$ . This type of saturation has also been observed in systems where the spin-orbit coupling length ( $l_{SO}$ ) becomes comparable to the phase breaking length [17]. We have extracted  $l_{SO}$  by using the full HLN equation [52, 53] (See supplementary information). The extracted  $l_{SO}$  is much smaller compared to  $l_\phi$  (as expected for TI systems) ruling out that possibility as well.

The most common reason, however, for the saturation of  $l_\phi$  is the presence of magnetic impurities or localized spins, which leads to the saturation even in extremely pure systems [22, 24, 25]. Experimental and theoretical

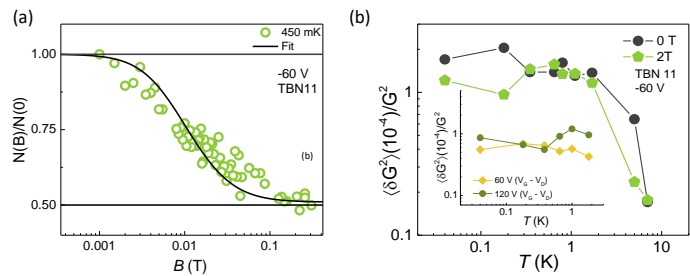


Figure 4. **Variation of UCF with magnetic field.** (a) Normalized UCF magnitude at  $V_G - V_D = 0$  V for 450 mK clearly exhibiting a factor of two reduction indicating the intrinsic preservation of time reversal symmetry in these systems. The solid line is fit to the data according to Eq. 4. (b) Normalized variance  $\langle \delta G^2 \rangle / \langle G^2 \rangle$  as function of  $T$  for  $B_\perp = 0$  T and 2 T at  $V_G - V_D = -60$  V. The qualitative nature of saturation does not change even upon the application of a high magnetic field, probably indicating that magnetic moments are not responsible for the saturation. Inset shows normalized variance at  $V_G - V_D = 60$  V and at 120 V, both showing similar saturation as a function of  $T$ .

studies have reported the presence of localized spins [54] or intrinsic magnetic instabilities in the TI surface [55]. One manifestation of the presence of magnetic impurities can be long- or short-range magnetic ordering, which can lead to the removal of TRS in the system. To probe this, we have measured  $\langle \delta G^2 \rangle$  as a function of  $B_\perp$  on TBN11. The magnitude of the conductance fluctuations is plotted as  $N_G(B)/N_G(0)$  ( $N_G = \langle \delta G^2 \rangle / \langle G^2 \rangle$  is the normalized variance) in Fig. 4(a). We observe a factor of two reduction in the normalized magnitude when  $B_\perp \gg B_\phi$  due to the suppression of the Cooperon contribution in transport and the crossover of the system from symplectic to unitary symmetry class, which indicates that TRS is intact intrinsically in these systems. For a quantitative understanding, the normalized magnitude has been fitted with the expression [16, 34, 36, 56]

$$\begin{aligned} N(B)/N(0) &= \frac{1}{2} + \frac{1}{b^2} \sum_{n=0}^{\infty} \frac{1}{[(n + \frac{1}{2}) + \frac{1}{b}]^{1.5}} \\ &= \frac{1}{2} - \frac{1}{2b^2} \Psi'' \left( \frac{1}{2} + \frac{1}{b} \right). \end{aligned} \quad (4)$$

Here  $b = 8\pi B(l_\phi)^2/(h/e)$ ,  $\Psi''$  is the double derivative of the digamma function, and  $l_\phi$  is the fitting parameter. The solid line in Fig. 4 (a) is the fit according to Eq. 4, which captures the variation with normalized magnitude with  $B$ . The  $l_\phi$  obtained from the fit is 220 nm, similar to  $l_\phi$  obtained from UCF and MR, which confirms the validity of the analysis and the factor of two reduction.

Spin-flip scattering due to the presence of unwanted magnetic impurities, e.g., due to finite purity of the metal components, may also cause dephasing. To investigate this, we have extracted  $\langle \delta G^2 \rangle$  as a function of  $T$  for  $B_\perp = 0$  T and 2 T at different  $V_G - V_D$ . The normalized

magnitude  $\langle \delta G^2 \rangle / G^2$  shows a saturation for both  $B_{\perp} = 0$  T and 2 T for  $T < 2$  K. The presence of a magnetic field  $B_{\perp} \gg k_B T / (g\mu_B)$  is expected to freeze the magnetic moments and suppress spin-flip scattering in the sample. Here  $k_B$ ,  $g$ , and  $\mu_B$  are the Boltzmann constant, Landé  $g$ -factor, and Bohr magneton respectively. The fact that the saturation persists even in the presence of  $B_{\perp}$ , indicates that it is not due to any magnetic impurities or localized spins in the system. To probe the effect of coupling between the surface states and charged disorders in the bulk, we have measured the conductance fluctuations for more positive gate voltages ( $V_G - V_D = 60$  V and 120 V). The number density at  $V_G - V_D = 120$  V is  $8.6 \times 10^{16} \text{ m}^{-2}$ , which corresponds to bulk transport dominated regime, where the coupling of the two surfaces and the bulk is also higher, compared to that near the Dirac point ( $-60$  V) [11, 57]. However, the nature of saturation also does not change for more positive gate voltages, implying that it is independent of the coupling between surface states and the charged puddles in the bulk (inset of Fig. 4b).

While the exact source of saturation remains unascertained, we discuss some plausible mechanisms that may lead to the saturation of  $l_{\phi}$  in TIs. The saturation can arise from the presence of two-level systems as has been explored in Ref. [58, 59]. Such two-level systems can arise from the charge fluctuations in the bulk, which are known to be the dominant source of  $1/f$  noise in TI [39, 40, 60]. The relaxation dynamics of these charged defects in the bulk can lead to a very weak dependence of  $l_{\phi}$  on  $T$ . We also note that the temperature where  $l_{\phi}$  saturates in M10 is  $\sim 300$  mK, which is an order of magnitude lower compared to the exfoliated samples (F7 and F10), and  $l_{\phi}^{sat}$  is also an order of magnitude higher. This difference in  $l_{\phi}^{sat}$  and  $T^{sat}$  between these samples, grown by totally different methods could be indicative of a lower charge

impurity driven inhomogeneity in the bulk in case of the MBE sample. Liao et al. have shown that the charge puddles in the bulk lead to a sublinear dependence of  $l_{\phi}$  on  $T$  [11]. It is possible that at low  $T$ , these uncompensated charges are strongly localized, leading to reduced screening of electromagnetic fluctuations. This can produce additional dephasing of the surface carriers, which might limit  $l_{\phi}$  to a finite value. Recently Väyrynen et al. have proposed back-scattering of electrons by electromagnetic fluctuations from the charge puddles in the bulk in 2D TIs [61]. The effect of such inelastic scattering on  $l_{\phi}$  in 3D TIs remains to be seen, and may also provide crucial insight into the factors leading to the saturation of  $l_{\phi}$  in topological insulators.

In conclusion, we have measured the Fermi energy and time-dependent conductance fluctuations and magnetoresistance to probe the sources of dephasing of the surface carriers in topological insulators. The phase breaking length obtained from both these techniques show a saturation below some specific temperatures which are sample dependent. We have eliminated several factors that may lead to the saturation of  $l_{\phi}$  such as finite-size effects, spin-orbit coupling length, and surface-bulk coupling. The magnetic field dependence of the conductance fluctuations also eliminates the possibility of the saturation arising due to the presence of magnetic impurities or localized spins in the system. Our work suggests an additional dephasing mechanism in TIs which is dominant at low temperatures, and limits the phase breaking length to a finite value at low temperatures.

S.I., S.B., D.S., and A.G. acknowledge support from DST, India. A.R., A.K., and N.S. acknowledge support from The Pennsylvania State University Two-Dimensional Crystal Consortium – Materials Innovation Platform (2DCC-MIP), which is supported by NSF cooperative Agreement No. DMR-1539916.

- 
- [1] M. Z. Hasan and C. L. Kane, Rev. Mod. Phys. **82**, 3045 (2010).
- [2] J. E. Moore, Nature **464**, 194 (2010).
- [3] M. König, S. Wiedmann, C. Brüne, A. Roth, H. Buhmann, L. W. Molenkamp, X.-L. Qi, and S.-C. Zhang, Science **318**, 766 (2007).
- [4] Y. Chen, J. G. Analytis, J.-H. Chu, Z. Liu, S.-K. Mo, X.-L. Qi, H. Zhang, D. Lu, X. Dai, and Z. Fang, Science **325**, 178 (2009).
- [5] C.-Z. Chang, J. Zhang, X. Feng, J. Shen, Z. Zhang, M. Guo, K. Li, Y. Ou, P. Wei, and L.-L. Wang, Science **340**, 167 (2013).
- [6] Y. S. Kim, M. Brahlek, N. Bansal, E. Edrey, G. A. Kapilevich, K. Iida, M. Tanimura, Y. Horibe, S.-W. Cheong, and S. Oh, Phys. Rev. B **84**, 073109 (2011).
- [7] R. Ockelmann, A. Müller, J. Hwang, S. Jafarpisheh, M. Drögeler, B. Beschoten, and C. Stampfer, Phys. Rev. B **92**, 085417 (2015).
- [8] J. Wang, A. M. DaSilva, C.-Z. Chang, K. He, J. Jain, N. Samarth, X.-C. Ma, Q.-K. Xue, and M. H. Chan, Phys. Rev. B **83**, 245438 (2011).
- [9] D. Zhang, A. Richardella, D. W. Rench, S.-Y. Xu, A. Kandala, T. C. Flanagan, H. Beidenkopf, A. L. Yeats, B. B. Buckley, P. V. Klimov, A. Yazdani, P. Schiffer, M. Hasan, Z. and N. Samarth, Phys. Rev. B **86**, 205127 (2012).
- [10] A. Kandala, A. Richardella, D. Zhang, T. C. Flanagan, and N. Samarth, Nano Lett. **13**, 2471 (2013).
- [11] J. Liao, Y. Ou, H. Liu, K. He, X. Ma, Q.-K. Xue, and Y. Li, Nat. Commun. **8**, 16071 (2017).
- [12] Z. Li, T. Chen, H. Pan, F. Song, B. Wang, J. Han, Y. Qin, X. Wang, R. Zhang, J. Wan, *et al.*, Sci. Rep. **2**, 595 (2012).
- [13] J. G. Checkelsky, Y. S. Hor, R. J. Cava, and N. Ong, Phys. Rev. Lett. **106**, 196801 (2011).
- [14] J.-J. Lin and J. Bird, J. Phys. Condens. Matter **14**, R501 (2002).
- [15] H. Steinberg, J.-B. Laloë, V. Fatemi, J. S. Moodera, and P. Jarillo-Herrero, Phys. Rev. B **84**, 233101 (2011).
- [16] S. Islam, S. Bhattacharyya, H. Nhalil, S. Elizabeth, and

- A. Ghosh, Phys. Rev. B **97**, 241412 (2018).
- [17] Y. K. Fukai, S. Yamada, and H. Nakano, Appl. Phys. Lett. **56**, 2123 (1990).
- [18] J. Lin and N. Giordano, Phys. Rev. B **35**, 1071 (1987).
- [19] J. Vranken, C. Van Haesendonck, and Y. Bruynseraede, Phys. Rev. B **37**, 8502 (1988).
- [20] P. Fournier, J. Higgins, H. Balci, E. Maiser, C. Lobb, and R. Greene, Phys. Rev. B **62**, R11993 (2000).
- [21] D. Pivin Jr, A. Andresen, J. Bird, and D. Ferry, Phys. Rev. Lett. **82**, 4687 (1999).
- [22] F. Schopfer, C. Bäuerle, W. Rabaud, and L. Saminadayar, Phys. Rev. Lett. **90**, 056801 (2003).
- [23] P. Mohanty, E. Jariwala, and R. A. Webb, Phys. Rev. Lett. **78**, 3366 (1997).
- [24] F. Pierre and N. O. Birge, Phys. Rev. Lett. **89**, 206804 (2002).
- [25] F. Pierre, A. Gougam, A. Anthore, H. Pothier, D. Esteve, and N. O. Birge, Phys. Rev. B **68**, 085413 (2003).
- [26] P. Mohanty and R. A. Webb, Phys. Rev. B **55**, R13452 (1997).
- [27] C. Chuang, L.-H. Lin, N. Aoki, T. Ouchi, A. M. Mahjoub, T.-P. Woo, R. K. Puddy, Y. Ochiai, C. Smith, and C.-T. Liang, Appl. Phys. Lett. **103**, 043117 (2013).
- [28] B. Huard, A. Anthore, N. O. Birge, H. Pothier, and D. Esteve, Phys. Rev. Lett. **95**, 036802 (2005).
- [29] S. Hikami, A. I. Larkin, and Y. Nagaoka, Prog. Theor. Phys. **63**, 707 (1980).
- [30] N. Birge, B. Golding, and W. Haemmerle, Phys. Rev. B **42**, 2735 (1990).
- [31] A. Ghosh and A. Raychaudhuri, Phys. Rev. Lett. **84**, 4681 (2000).
- [32] A. Ghosh, S. Kar, A. Bid, and A. Raychaudhuri, arXiv preprint cond-mat/0402130 (2004).
- [33] P. A. Lee and A. D. Stone, Phys. Rev. Lett. **55**, 1622 (1985).
- [34] P. Lee, A. D. Stone, and H. Fukuyama, Phys. Rev. B **35**, 1039 (1987).
- [35] A. N. Pal, V. Kochat, and A. Ghosh, Phys. Rev. Lett. **109**, 196601 (2012).
- [36] S. Shamim, S. Mahapatra, G. Scappucci, W. Klesse, M. Simmons, and A. Ghosh, Sci. Rep. **7** (2017).
- [37] A. Taskin, Z. Ren, S. Sasaki, K. Segawa, and Y. Ando, Phys. Rev. Lett. **107**, 016801 (2011).
- [38] C. R. Dean, A. F. Young, I. Meric, C. Lee, L. Wang, S. Sorgenfrei, K. Watanabe, T. Taniguchi, P. Kim, and K. L. Shepard, Nat. Nanotechnol. **5**, 722 (2010).
- [39] S. Bhattacharyya, A. Kandala, A. Richardella, S. Islam, N. Samarth, and A. Ghosh, Appl. Phys. Lett. **108**, 082101 (2016).
- [40] S. Islam, S. Bhattacharyya, A. Kandala, A. Richardella, N. Samarth, and A. Ghosh, Appl. Phys. Lett. **111**, 062107 (2017).
- [41] L. Bao, L. He, N. Meyer, X. Kou, P. Zhang, Z.-G. Chen, A. V. Fedorov, J. Zou, T. M. Riedemann, and T. A. Lograsso, Sci. Rep. **2**, 726 (2012).
- [42] R. Gorbachev, F. Tikhonenko, A. Mayorov, D. Horsell, and A. Savchenko, Phys. Rev. Lett. **98**, 176805 (2007).
- [43] J. H. Scofield, Rev. Sci. Instrum **58**, 985 (1987).
- [44] N. O. Birge, B. Golding, and W. Haemmerle, Phys. Rev. Lett. **62**, 195 (1989).
- [45] A. Trionfi, S. Lee, and D. Natelson, Phys. Rev. B **70**, 041304 (2004).
- [46] E. Akkermans and G. Montambaux, *Mesoscopic physics of electrons and photons* (Cambridge University Press, 2007).
- [47] P. Adroguer, D. Carpentier, J. Cayssol, and E. Orignac, New J. Phys. **14**, 103027 (2012).
- [48] C. Beenakker and H. van Houten, in *Solid State Phys.*, Vol. 44 (Elsevier, 1991) pp. 1–228.
- [49] S. Morozov, K. Novoselov, M. Katsnelson, F. Schedin, L. Ponomarenko, D. Jiang, and A. Geim, Phys. Rev. Lett. **97**, 016801 (2006).
- [50] X. Wu, X. Li, Z. Song, C. Berger, and W. A. de Heer, Phys. Rev. Lett. **98**, 136801 (2007).
- [51] M. Liu, C.-Z. Chang, Z. Zhang, Y. Zhang, W. Ruan, K. He, L.-l. Wang, X. Chen, J.-F. Jia, S.-C. Zhang, *et al.*, Phys. Rev. B **83**, 165440 (2011).
- [52] S. Zhang, R. McDonald, A. Shekhter, Z. Bi, Y. Li, Q. Jia, and S. T. Picraux, Appl. Phys. Lett. **101**, 202403 (2012).
- [53] R. Dey, T. Pramanik, A. Roy, A. Rai, S. Guchhait, S. Sonde, H. C. Movva, L. Colombo, L. F. Register, and S. K. Banerjee, Appl. Phys. Lett. **104**, 223111 (2014).
- [54] D. Nisson, A. Dioguardi, P. Klavins, C. Lin, K. Shirer, A. Shockley, J. Crocker, and N. Curro, Phys. Rev. B **87**, 195202 (2013).
- [55] Y. Baum and A. Stern, Phys. Rev. B **85**, 121105 (2012).
- [56] A. D. Stone, Phys. Rev. B **39**, 10736 (1989).
- [57] D. Kim, S. Cho, N. P. Butch, P. Syers, K. Kirshenbaum, S. Adam, J. Paglione, and M. S. Fuhrer, Nat. Phys. **8**, 459 (2012).
- [58] Y. Imry, H. Fukuyama, and P. Schwab, EPL **47**, 608 (1999).
- [59] A. Aleshin, V. Kozub, D.-S. Suh, and Y. Park, Phys. Rev. B **64**, 224208 (2001).
- [60] S. Bhattacharyya, M. Banerjee, H. Nhalil, S. Islam, C. Dasgupta, S. Elizabeth, and A. Ghosh, ACS Nano **9**, 12529 (2015).
- [61] J. I. Väyrynen, D. I. Pikulin, and J. Alicea, Phys. Rev. Lett. **121**, 106601 (2018).